Hesperetin induces apoptosis in A549 cells via the Hsp70-mediated activation of Bax

MASAYA TANAKA, HIROSHI ENDO, KONATSU SAKUSA and MIHIRO YANO

Department of Nutrition, School of Human Cultures, The University of Shiga Prefecture, Hikone, Shiga 522-8533, Japan

Received June 8, 2022; Accepted September 14, 2022

DOI: 10.3892/ijo.2022.5433

Abstract. Hesperetin, a predominant flavonoid found in citrus fruits, has received considerable attention for its potential anticancer activity through the reduction of cell viability and the induction of apoptosis. Several effector mechanisms have been demonstrated underlying the antitumor properties of hesperetin but its specific mechanisms have not yet been fully elucidated. In the present study, how hesperetin affects the proliferation of A549 cells and the related cell proliferation regulatory mechanisms, were inevstigated. To elucidate the mechanisms underlying the effects of hesperetin on A549 cells, MTT assay, colony formation assay, flow cytometry, immunoblotting, reverse transcription-quantitative PCR and JC-1 staining were performed. The data revealed that hesperetin inhibited cell proliferation and induced apoptosis in these cells. Hesperetin also decreased the level of heat shock protein 70 (Hsp70), a negative regulator of the mitochondrial apoptosis pathway, often overexpressed in various cancer cells and suspected to contribute to tumor development. Hesperetin-induced Hsp70 suppression was associated with reduced cytosolic Bax and increased mitochondrial Bax levels, leading to the enhancement of the mitochondrial apoptotic cascade. The Hsp70 overexpression-induced reduction in the level of hesperetin-induced apoptosis provides evidence to hesperetin-induced apoptosis being mediated by affecting Hsp70. Furthermore, it was demonstrated that hesperetin reduced Hsp70 expression by inducing a proteasome-mediated degradation via the upregulation of E3-ligase, C-terminus of Hsp70-interacting protein (CHIP). The present study highlighted the importance of the Bax activation-triggered mitochondria-mediated pathway for hesperetin-induced apoptosis and demonstrated a novel mechanism of how Hsp70 played a critical role in the negative regulation of this apoptotic network in cancer cells.

Correspondence to: Professor Mihiro Yano, Department of Nutrition, School of Human Cultures, The University of Shiga Prefecture, 2500 Hassaka-cho, Hikone, Shiga 522-8533, Japan
E-mail: yano.m@shc.usp.ac.jp

Key words: hesperetin, cancer, Hsp70, Bax, apoptosis, ubiquitin-proteasome

Introduction

An imbalance between cell proliferation and death is the primary cause of cancer. The absence of apoptotic signals inhibits cell death, leading to uncontrolled cell proliferation and cancer (1,2). Cancer cells often express several proteins that, when abnormally elevated, render tumor cells resistant to apoptosis (3,4). Stress-inducible heat shock protein 70 (Hsp70; also called Hsp72), a member of the human Hsp70 family playing critical roles in cell survival under stressful conditions, is often overexpressed in cancer cells; the selective survival advantage that it confers may contribute to tumor formation (5-7). Interestingly, Hsp70 expression in certain cancer types has been correlated with poor prognosis and resistance to chemotherapy (8-10). Thus, reducing the levels of Hsp70 in cancer cells may be an effective means to prevent tumor progression. Hsp70 has been targeted with pharmaceuticals, such as triptolide, quercetin, and KNK437, which downregulate its expression (11-13). Hesperetin, a flavanone found in citrus fruits such as oranges and grapefruits, has various biological and pharmacological activities, including anti-inflammatory, antioxidant, antihypertension, and lipid-lowering effects (14,15). Hesperetin has been extensively studied for its anticancer properties associated with the inhibition of cell proliferation, cell cycle progression, and angiogenesis and the activation of apoptosis (16-18). Accumulated data have shown a marked ability of hesperetin to induce apoptosis in cancer cells through multiple target molecules and associated signaling pathways, such as ASK1/JNK, p38/MAPK, Notch1, ROS, Bcl-2 family members, and death receptors (19-24). The transduction of these hesperetin-induced apoptotic signals eventually results in mitochondrial outer membrane permeability, which is a key step in intrinsic apoptosis.

The intrinsic mitochondria-mediated apoptosis pathway is regulated by Bcl-2 family members, including proapoptotic (Bax, Bak, Bad, Bid and Bim) and antiapoptotic (Bcl-2 and Bcl-X_L) molecules. Although several lines of evidence have indicated that hesperetin modulates the levels of Bax and Bcl-2 in human cancer cell lines, leading to mitochondrial membrane disruption and apoptosis (20,22,23), it is not clear how hesperetin activates Bax and increases the Bax/Bcl-2 ratio. Targeting Hsp70, which is critical regulator of Bcl-2 family members, and thereby disposing cancer cells toward apoptosis have been described previously in the literature. Previous studies have confirmed not only that Hsp70 is

cytoprotective, but also that it interferes effectively with cell death induced by a wide variety of stimuli, including several cancer-related stresses. In addition to the function of Hsp70 as a potent inhibitor of the stress-activated kinase pathway that apparently blocks apoptotic signals via interactions with JNK, Ask1, and SEK1 (25-27), it has been well-documented that Hsp70 is also a negative regulator of the mitochondrial pathway of apoptosis. Studies on the antiapoptotic function of Hsp70 have focused on events that occur after mitochondrial disruption. Hsp70 prevents the recruitment of procaspase-9 to the apoptosome and its functional complex formation by direct interaction with apoptotic protease-activating factor 1 (28,29). Conversely, several studies have reported that Hsp70 can prevent apoptosis upstream of the mitochondria by inhibiting events that ultimately permeabilize the mitochondrial outer membrane, such as the activation of Bax. Hsp70 directly binds to Bax and prevents its translocation to the outer mitochondrial membrane where it promotes cell death (30,31). Therefore, the hesperetin-induced apoptosis via Bax prompted the investigation of whether or not Hsp70 is a target in hesperetin-induced apoptosis in cancer cells.

Materials and methods

Materials. Mouse monoclonal antibody against Hsp70 (cat. no. SMC-100) was purchased from Stress Marq Biosciences, Inc. Goat polyclonal antibody, anti-voltage-dependent anion channel (VDAC) (product code ab37985), and rabbit polyclonal antibody anti-STUB1/CHIP (product code ab134064) were obtained from Abcam. Rabbit anti-Bax (product no. 5023), anti-active caspase-9 (product no. 9502), anti-ubiquitin (product no. 3936), anti-MEK1/2 (product no. 8727), and anti-poly (ADP-ribose) polymerase (PARP; active-PARP) (product no. 9542) antibodies were purchased from Cell Signaling Technology, Inc. The mouse monoclonal antibody against β-actin (cat. no. 017-24551) and MG132 (cat. no. 139-18451) were obtained from FUJIFILM Wako Pure Chemical Corporation. Hesperetin (cat. no. H4125) and all other chemicals used in this study were purchased from Sigma-Aldrich; Merck KGaA.

Cell culture and viability assay. A549 lung cancer cell line (JCRB no. JCRB0076) was obtained from NIBIOHN. H358 lung cancer cell line (ATCC no. CRL-5807) was from the American Type Culture Collection. Both cancer cell lines were cultured in Dulbecco's modified Eagle's medium containing 10% fetal bovine serum at 37˚C. Hesperetin was dissolved in dimethyl sulfoxide. Briefly A549 or H358 cells were seeded at $5x10^5$ cells/well in 12-well plates for 24 h at 37˚C. A549 cells were treated with various concentrations of hesperetin (0, 100, 200, 300, 400, 500, 600, 700, 800, 900, and 1,000 μM) for 48 h at 37˚C. In addition, H358 cells were treated with various concentrations of hesperetin (0, 200, 400 and 600 μM) for 48 h at 37˚C. Mitochondrial dehydrogenase 3-(4,5-dimethylthiazol-2-yl)-2,5-diphenyltetra-zolium bromide (MTT) assay was used to assess cell death/survival. The cells were incubated for 2 h with MTT solution at 37˚C and then 50% iso-propanol/10% SDS was added to dissolve the formazan. The reaction product was measured by spectrophotometry at a wavelength of 570 nm, and the relative viability of cells treated with hesperetin vs. untreated cells was calculated. Cell viability was used to calculate the half maximal inhibitory concentration (IC_{50}). In addition, to study the molecular mechanism of Hsp70, A549 cells were pretreated with the proteasome inhibitor MG132. MG132 (3 μM) was added to A549 cells for 2 h at 37˚C, before exposure to hesperetin.

Colony formation assay. A549 cells were plated in a 12-well plate at a density of 1,000 cells/well for 24 h before treatment with various concentrations of hesperetin (0, 200, 400, and 600 μM) for 48 h at 37˚C. Following treatment, cells were incubated in fresh media for 7 days. Colonies were fixed with 4% paraformaldehyde for 20 min at room temperature and visualized using 0.05% crystal violet solution for 20 min at room temperature. A colony was defined as an agglomeration of >50 cells. After washing, the ColonyArea (version Dec 22, 2016) (https://b2share.eudat.eu/records/39fa39965b314f658e4a198a78d7f6b5), a plugin for ImageJ software (version 1.53s; National Institutes of Health), was used for quantification.

Cell cycle analysis. A549 cells were cultured in a 60-mm dish at a density of $2x10^5$ cells/dish. The cells treated with various concentrations of hesperetin (0, 200, 400, and 600 μM) for 48 h at 37˚C were fixed with 70% ethanol at -20˚C for 2 h and stained with a propidium iodide (PI) concentration of 0.05 mg/ml for 30 min at 37˚C. Fluorescence was measured using FACSCalibur (BD Biosciences), and data were analyzed using CellQuest software (version 3.1; BD Biosciences).

Quantification of apoptosis by flow cytometry. A549 cells were seeded at $5x10^5$ cells/dish in a 60-mm dish. The cells were washed with Annexin V staining buffer [10 mM HEPES (pH 7.4), 150 mM NaCl, 5 mM KCl, 1 mM $MgCl_2$, and 1.8 mM CaCl2] and incubated with CF488A-Annexin V and PI (cat. no. 15342-54; Nacalai Tesque, Inc.) in a staining buffer for 30 min at 37˚C in the dark. Fluorescence was measured using FACSCalibur, and data were analyzed using CellQuest software (version 3.1).

Immunoblotting and cell fractionation. A549 cells were cultured in a 60-mm dish at a density of $2x10^5$ cells/dish. The cells were lysed using immunoprecipitation assay buffer [50 mM Tris-HCl (pH 7.5), 150 mM NaCl, 1 mM EDTA, and 0.1% NP-40] containing Protease Inhibitor Cocktail Set (Nacalai Tesque, Inc.). The cell lysates were resolved in Laemmli sample buffer. The concentration of total protein was measured using a BCA assay. The samples (20 μg protein/lane) were subjected to 10% sodium dodecyl sulfate-polyacrylamide gel electrophoresis (SDS-PAGE), transferred onto a polyvinylidene difluoride membrane. The membranes were blocked with 10% skim milk in TBS-0.1% Tween-20 buffer for 2 h at room temperature, and then reacted with the respective antibodies: Hsp70 (1:1,000), VDAC (1:500), CHIP (1:5,000), Bax (1:1,000), caspase-9 (1:1,000), ubiquitin (1:1,000), MEK1/2 (1:1,000), PARP (1:1,000) and β-actin (1:5,000) overnight at 4˚C. The membranes were treated with the secondary antibodies conjugated with horseradish peroxidase (HRP) (1:4,000; cat. nos. HAF007, HAF109, and HAF008; R&D systems) for 1 h at room temperature and detected with an ECL chemiluminescence detection kit (GE Healthcare; Cytiva).

A549 cells ($2x10^5$ cells/dish in 100 mm dish) lysed in 20 mM HEPES-KOH (pH 7.5) buffer containing 0.25 M sucrose were homogenized in a Dounce homogenizer and centrifuged at 1,000 x g for 30 min at 4˚C to separate nuclei and unbroken cells. The supernatants were centrifuged at 10,000 x g for 15 min at 4˚C, and the pellets were collected as the heavy membrane/mitochondrial fraction. The cytosolic fractions were isolated according to the manufacturer's protocol, using the Mitochondria Isolation Kit for Cultured Cells (cat. no. 89874) from Thermo Fisher Scientific, Inc.

Immunoprecipitation. For the immunoprecipitation, the cell lysates were incubated with 5 μg Hsp70 antibody (cat. no. SPC-103; Stress Marq Bioscience, Inc.) overnight at 4˚C. Subsequently, 20 μl of Protein G-sepharose beads (cat. no. P3296; Sigma-Aldrich; Merck KGaA) were added to collect the immunocomplexes for an additional 1 h of incubation at 4˚C. The pellets were washed three times with assay buffer by centrifugation at 1,000 x g for 5 min at 4˚C. The supernatant was discarded, and the beads were resuspended with 40 μl of electrophoresis buffer and analyzed by SDS-PAGE and immunoblotting using an anti-ubiquitin (cat. no. 3936; Cell Signaling technology, Inc.) or anti-Hsp70 (cat. no. SMC-100; Stress Marq Bioscience, Inc.) antibody.

Overexpression of Hsp70. A549 cells ($2x10^5$ cells/dish in a 60-mm dish) were seeded into 12-well plates for 24 h before transfection. The expression plasmid of pCMV-Tag3B myc-Hsp70 was supplied by Dr Tohru Ichimura (Laboratory of Cell Molecular Biology, Department of Applied Chemistry, National Defense Academy, Yokosuka, Japan). The negative control plasmid, pCMV (an empty vector), was supplied from RIKEN BioResource Center. Transfection was performed with 8 μg vector using Lipofectamine 3000 (Thermo Fisher Scientific, Inc.) in accordance with the manufacturer's instructions. The cells were incubated for 12 h at 37˚C, and subsequently treated with hesperetin for 48 h.

RNA extraction and reverse transcription-quantitative PCR (RT-qPCR). Total RNA from cells was extracted using QIAshredder and RNeasy Mini Kit (Qiagen GmbH) according to manufacturer's protocol. The cDNA synthesis was performed by High-Capacity RNA-to-cDNA™ Kit (Thermo Fisher Scientific Inc.) and qPCR was subsequently performed on QuantStudio® 5 Real-Time PCR (Thermo Fisher Scientific Inc.) system using PowerUp™ SYBR™ Green Master Mix (Thermo Fisher Scientific, Inc.). The reaction was carried out according to the following amplification protocol: 95˚C for 2 min, 40 cycles at 95˚C for 15 sec, 60˚C for 1 min and 95˚C for 15 sec. Gene expression was analyzed according to the $2^{-\Delta\Delta Cq}$ method (32). The following sequences of the primers were used, respectively: Hsp70 forward primer (F), 5'-GCCGAG AAGGACGAGTTTGA-3' and reverse primer (R), 5'-TCC GCTGATGATGGGGTTAC-3'; β-actin (F), 5'-ATGTGGCCG AGGACTTTGATT-3' and (R), 5'-AGTGGGGTGGCTTTT AGGATG-3'.

Knockdown of CHIP. The specific small interfering RNA (siRNA) for CHIP was obtained from Ajinomoto Bio-Pharma: siCHIP sequence of the sense strand (5'-AGGCCAAGCACGACAAGUAdTdT-3'). The negative control siRNA (MISSION siRNA Universal Negative Control #1; cat. no. SIC001) was purchased from Merck KGaA. A549 cells were transfected with siRNA (10 nmol/l) using Lipofectamine RNAi MAX (Thermo Fisher Scientific). The cells were then incubated for 24 h at 37˚C, and subsequently treated with 600 μM of hesperetin and grown for 48 h at 37˚C to allow an effective decrease in the expression of the respective target molecules. For the MTT assay, A549 cells were treated with various concentrations of hesperetin (0, 200, 400 and 600 μM) for 48 h at 37˚C.

JC-1 staining. Mitochondrial permeability transition was determined by staining the cells with 5,5',6,6'-tetrachloro-1,1,3,3'-tetraethyl-benzimidazolyl-carbocyanin iodide (JC-1; Molecular Probes; Invitrogen; Thermo Fisher Scientific, Inc.) for 2 h at 37˚C in the dark. The cells were subsequently washed with assay buffer in accordance with the manufacturer's protocol and immediately imaged using a fluorescence microscope (Keyence Corporation) with the red (λexcitation: 560±40 nm band pass filter, λdetection: 630±60 nm band pass filter) and green (λexcitation: 470±40 nm band pass filter, λdetection: 535±50 nm band pass filter) fluorescence channels.

Statistical analysis. The data were expressed as the mean ± standard deviation (SD) for three independent experiments. Comparisons between quantitative variables were assessed using one-way ANOVA followed Tukey's post hoc test. $P<0.05$ was considered to indicate a statistically significant difference.

Results

Hesperetin inhibits proliferation and induces apoptosis in lung cancer cell lines. The survival of lung cancer cells treated with hesperetin was assessed using an MTT assay. Following treatment with hesperetin, the viability of A549 (Fig. 1A) and H358 (Fig. 1B) lung cancer cell lines decreased in a concentration-dependent manner. The IC_{50} value of the potential cytotoxic effects of hesperetin against A549 was 520 μM (Fig. 1A). To further examine the effect of hesperetin on A549 cell proliferation, a colony formation assay was performed. Hesperetin markedly reduced the colonigenic potential of A549 cells in a dose-dependent manner (Fig. 1C). The colony formation measured by percent area of the colonies with hesperetin treatments of 400 and 600 μM were 68 and 30%, respectively, when that of the control without hesperetin was set at 100%. These results were not significantly different from those of the MTT assay. Cell cycle analysis was performed with a flow cytometer to examine the inhibitory effect of hesperetin on lung cancer cells. As shown in Fig. 1D, the cell cycle progression of A549 cells revealed no significant change after treatment with various concentrations of hesperetin. Considering that hesperetin did not affect cell cycle progression, it was then investigated whether or not the inhibitory effects of hesperetin on A549 cell viability are induced via apoptotic cell death. Apoptotic cell death was assessed using CF488A-Annexin V through flow cytometry. The increase in the number of apoptotic cells in hesperetin-treated cultures indicated that hesperetin decreased cell viability through apoptosis (Fig. 1E).

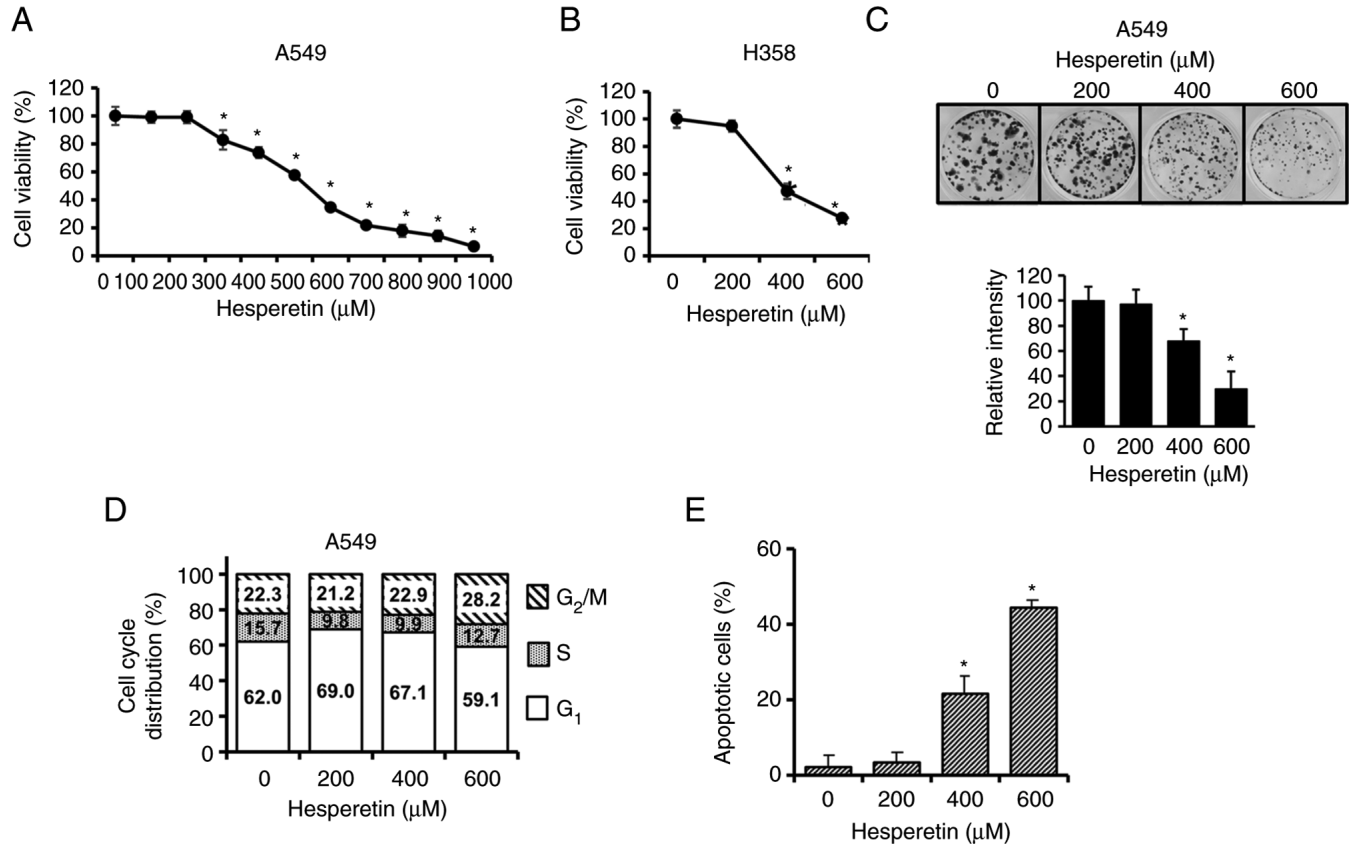

Figure 1. Hesperetin inhibits proliferation and induces apoptosis in lung cancer cell lines. The viabilities of (A) A549 cells and (B) H358 cells treated with hesperetin for 48 h were analyzed by MTT assay. Cell viability is represented as the percentage of cell viability without hesperetin, which was set at 100%. (C) Colony formation assays of A549 cells treated with various doses of hesperetin for 48 h. A representative experiment out of three performed with similar results is shown (upper panel). The area covered by colonies was quantified (lower panel). (D) Effects of hesperetin on cell cycle distribution. A549 cells were treated with various concentrations of hesperetin for 48 h, and cell cycle phases were analyzed by flow cytometer. (E) Apoptotic cell death was assessed by flow cytometric analysis with fluorescein-isothiocyanate-conjugated Annexin V/PI staining at 48 h to observe hesperetin-induced apoptosis in A549 cells. Data indicate the mean ± standard deviation of three experiments. $^{*}P<0.01$ indicates a statistically significant difference from the respective control (without hesperetin).

Hesperetin induces mitochondria-dependent apoptosis associated with the activation of Bax in A549 cells. Several studies have shown that mitochondria and pro-apoptotic molecule, Bax, may be a direct and important target of hesperetin in sensitive cells (19,20,22,23,33). It was examined whether or not hesperetin promotes mitochondria-dependent apoptosis by inducing Bax translocation in A549 cells. Mitochondrial fractions were prepared from A549 cells incubated with or without hesperetin and immunoblotted for Bax in these fractions. In the presence of hesperetin, Bax was localized to the mitochondria in a dose-dependent manner, whereas hesperetin slightly reduced the amount of cytosolic Bax (Fig. 2A). Apoptotic signal transmission to the mitochondria leads to the activation of caspase-9, which then converts procaspase-3 into active caspase-3, resulting in PARP cleavage and apoptosis (34,35). The activation of caspase-9 and cleavage of PARP in A549 cells treated with hesperetin was assessed to examine whether or not hesperetin influences downstream mitochondrial-related apoptotic events. As shown in Fig. 2B, hesperetin induced the cleavage of caspase-9 in a concentration-dependent manner in A549 cells. Hesperetin also caused an increase in the level of cleaved PARP (Fig. 2B).

Hesperetin induces apoptosis by suppressing Hsp70 in A549 cells. Hsp70 was then investigated, which generally interacts with Bax to prevent its translocation to the mitochondria in living cells and inhibits cell death, to clarify the molecular mechanism that underlies the activation of Bax in hesperetin-induced apoptosis (30,31). The expression of Hsp70 after the exposure of A549 cells to various concentrations of hesperetin was analyzed by immunoblotting to examine the effects of hesperetin on Hsp70. Hesperetin significantly decreased the expression level of Hsp70 in A549 cells (Fig. 3A). The expression of Hsp70 was overexpressed as a myc-tagged protein in A549 cells (Fig. 3B) and its effect on the decrease of cell viability induced by hesperetin was assessed to ascertain the effects of Hsp70 expression on cell death while excluding all the effects of hesperetin unrelated to Hsp70. As revealed in Fig. 3C, Hsp70 overexpression rescued A549 cells from hesperetin-induced apoptosis compared to cells transfected with the empty vector. It was next examined whether or not the forced expression of Hsp70 prevents the translocation of Bax to mitochondria caused by hesperetin. In A549 cells with exogenously overexpressed Hsp70, Bax localization to the mitochondria in the presence of increasing doses of hesperetin significantly decreased as compared to that in the cells with endogenous expression of Hsp70 (Figs. 2A and 3D). These observations indicated that hesperetin promoted the apoptotic signal at the Bax activation step of the mitochondrial apoptotic

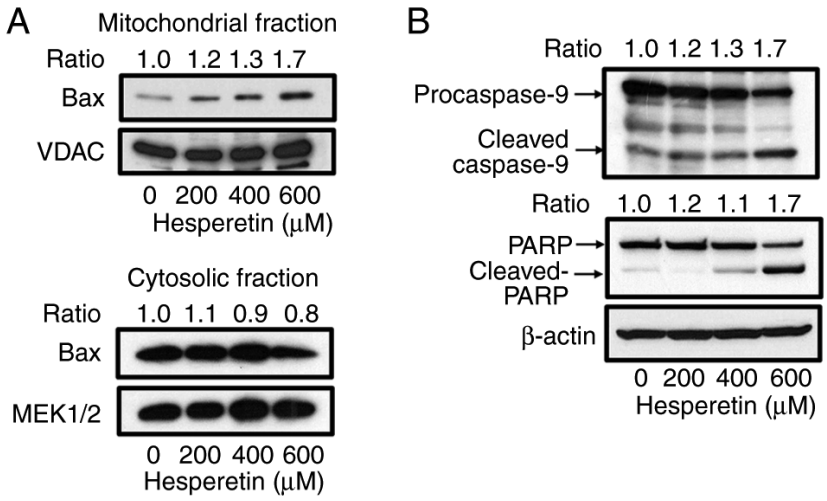

Figure 2. Hesperetin induces mitochondria-dependent apoptosis associated with the activation of Bax in A549 cells. (A) A549 cells, treated with hesperetin, were lysed and fractionated by differential centrifugation to separate the mitochondria from the cytosol. The translocation of Bax to the mitochondria was visualized by immunoblotting of the mitochondrial fraction using an anti-Bax antibody (upper panel). VDAC was used as a loading control to ensure the use of equal amounts of mitochondria in each lane. The quantity of Bax was estimated by densitometric analysis. Ratios of Bax band intensities normalized to VDAC band intensities are shown above the blots. Cytosolic Bax is presented in the lower panel. Equal loading of cytosolic fractions was controlled by MEK1/2. Ratios of Bax band intensities normalized to MEK1/2 band intensities are presented above the blots. (B) A549 cells were treated with hesperetin, and cell extracts were immunoblotted to detect the expression levels of full-length and cleaved caspase-9 and PARP. Ratios of cleaved caspase-9 and cleaved PARP band intensities normalized to β-actin band intensities are shown above the blots. The results presented are representative of three separate experiments. VDAC, voltage-dependent anion channel; PARP, poly (ADP-ribose) polymerase.

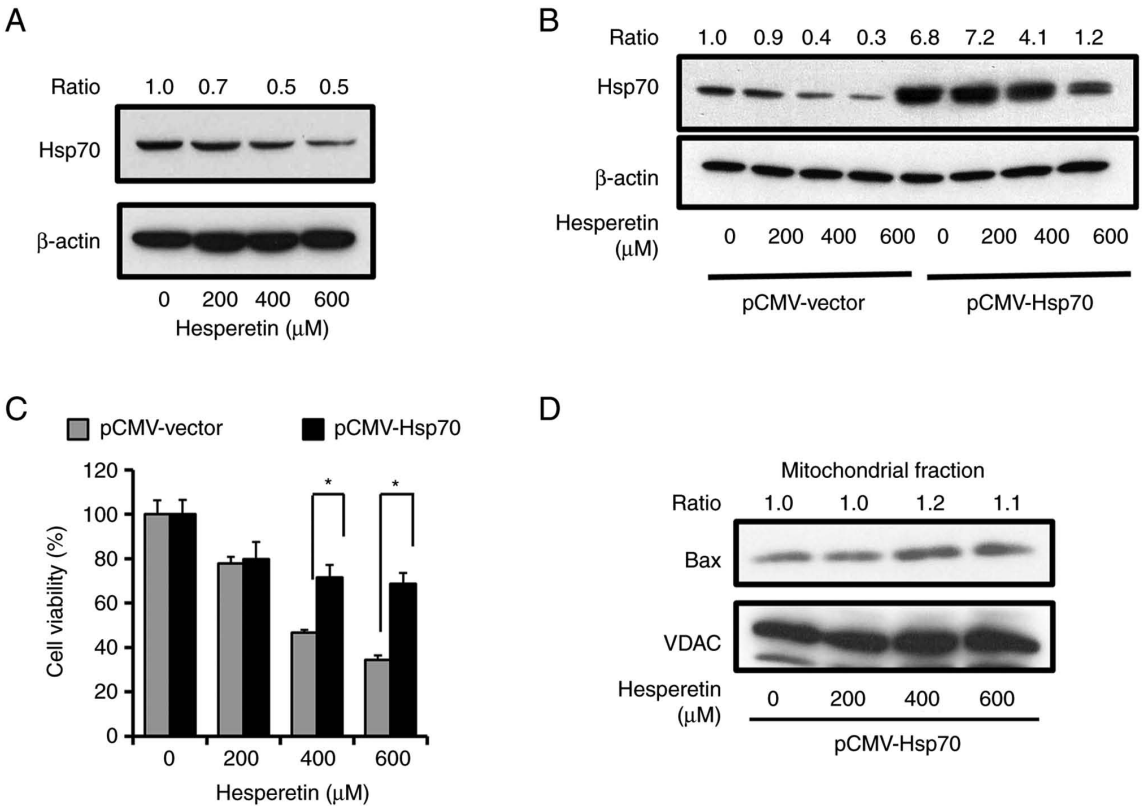

Figure 3. Involvement of Hsp70 in the apoptosis of A549 cells induced by hesperetin. (A) Downregulation of Hsp70 expression by hesperetin. Extracts prepared from A549 cells treated with hesperetin at the specified concentrations for 48 h were separated by SDS-PAGE and immunoblotted with an anti-Hsp70 antibody. The quantity of Hsp70 was estimated by densitometric analysis. Ratios of Hsp70 band intensities normalized to β-actin band intensities are shown above the blots. (B) A549 cells were transfected with pCMV-Tag3B myc-Hsp70 and pCMV-vector control treated with various concentrations of hesperetin for 48 h. Expression of Hsp70 was assessed by immunoblotting using an anti-Hsp70 antibody. Ratios of Hsp70 band intensities normalized to β-actin band intensities are shown above the blots. (C) Viabilities of A549 cells expressing myc-Hsp70 or vector control treated with hesperetin for 48 h were analyzed by MTT assay. Cell viability is represented as the percentage of cell viability without hesperetin, which was set at 100%. The data represent mean values of three separate experiments. Results are shown as mean ± SD, $^{*}P<0.01$. (D) A549 cells with exogenously overexpressed Hsp70, treated with hesperetin, were fractionated into mitochondria, and the translocation of Bax was analyzed by immunoblotting, using an anti-Bax antibody. Ratios of Bax band intensities normalized to VDAC band intensities are shown above the blots. Hsp70, heat shock protein 70; VDAC, voltage-dependent anion channel.

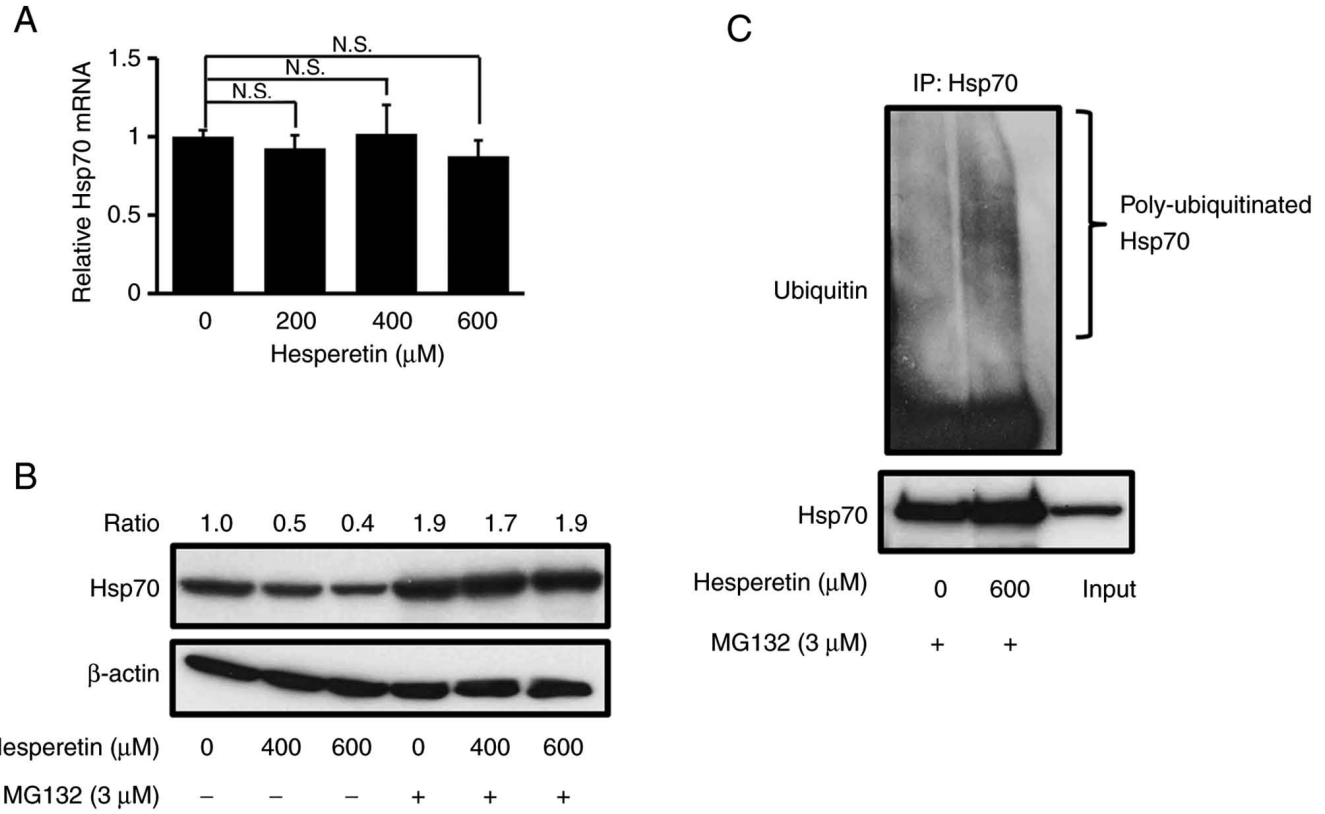

Figure 4. Hesperetin induces the proteasome-mediated degradation of Hsp70 in A549 cells. (A) The mRNA level of Hsp70 in A549 cells after treatment with hesperetin was determined by reverse transcription-quantitative PCR. (B) Prevention of decrease in Hsp70 expression by the proteasome inhibitor MG132 in hesperetin-treated A549 cells. Effects of MG 132 on Hsp70 expression. Cell extracts from A549 cells, untreated or treated, for 120 min at 37˚C with 3 μM MG132 before exposure to hesperetin, were separated by SDS-PAGE and immunoblotted with an anti-Hsp70 antibody. Ratios of Hsp70 band intensities normalized to β-actin band intensities are shown above the blots. (C) Ubiquitination of Hsp70 induced by hesperetin in the presence or absence of MG132. A549 cells were treated with 600 μM hesperetin in the presence or absence of 3 μM MG132. Hsp70 was immunoprecipitated with an anti-Hsp70 antibody and assessed by immunoblotting with an anti-ubiquitin antibody. Data are representative of three experiments. Hsp70, heat shock protein 70.

pathway via Hsp70 suppression, potentially contributing to the ability of hesperetin to inhibit A549 cell proliferation.

Hesperetin decreases Hsp70 expression by inducing a proteasome-mediated degradation. The mechanisms by which hesperetin decreases Hsp70 expression are poorly known. The expression of Hsp70 was examined at the mRNA level in A549 cells by RT-qPCR after treatment with hesperetin (Fig. 4A). The absence of a decrease in the mRNA level of Hsp70 following hesperetin treatment suggests that hesperetin causes its degradation in A549 cells. It is noteworthy that Hsp70 can often serve as a proteasome substrate and that it is stabilized by inhibition of the proteasome (36,37). To study the machinery that turns over Hsp70, A549 cells were pretreated with the proteasome inhibitor MG132 before exposure to hesperetin. The total amount of Hsp70 was nearly the same in the absence of hesperetin, regardless of cell exposure to MG132. MG132 prominently blocked the hesperetin-dependent decrease in Hsp70 expression in A549 cells (Fig. 4B). These observations indicated that hesperetin induced Hsp70 degradation by the proteasome. Based these observations, the ubiquitination of Hsp70 was further assessed. In the presence of MG132, hesperetin substantially increased the level of Hsp70 ubiquitination compared with control cells (Fig. 4C). Overall, these data clearly indicated that hesperetin promoted the proteasome-mediated degradation of Hsp70 in A549 cells.

Hesperetin induces the proteasome-mediated degradation of Hsp70 by increasing CHIP, leading to A549 cell apoptosis. CHIP has been demonstrated, *in vitro* and *in vivo*, to be associated with Hsp70 and ubiquitinate it, targeting it to the proteasome for degradation (36,37). The effect of hesperetin on CHIP in A549 cells was first investigated to clarify the mechanisms of CHIP responsible for the degradation of Hsp70. Interestingly, the level of CHIP markedly increased after hesperetin treatment in a concentration-dependent manner (Fig. 5A). Blockage of Hsp70 inhibition by the treatment of A549 cells with MG132 and the upregulation of CHIP in the presence of hesperetin suggested that Hsp70 was targeted by hesperetin for degradation by the proteasome. To further determine the functional importance of CHIP in the proteasome-mediated degradation of Hsp70 by hesperetin, the amount of endogenous CHIP present in A549 cells was attenuated with RNAi and its effects on Hsp70 expression were studied. Treatment with CHIP dsRNA did not cause the decrease in Hsp70 levels mediated by hesperetin compared with that measured in cells treated with scrambled siRNA (Fig. 5B). It was then examined how a selective knockdown of CHIP affects the survival of A549 cells exposed to increasing concentrations of hesperetin. As revealed in Fig. 5C, an MTT assay indicated that the inhibitory effect of hesperetin on the viability of A549 cells significantly decreased after CHIP silencing. This finding was consistent with the result of JC-1

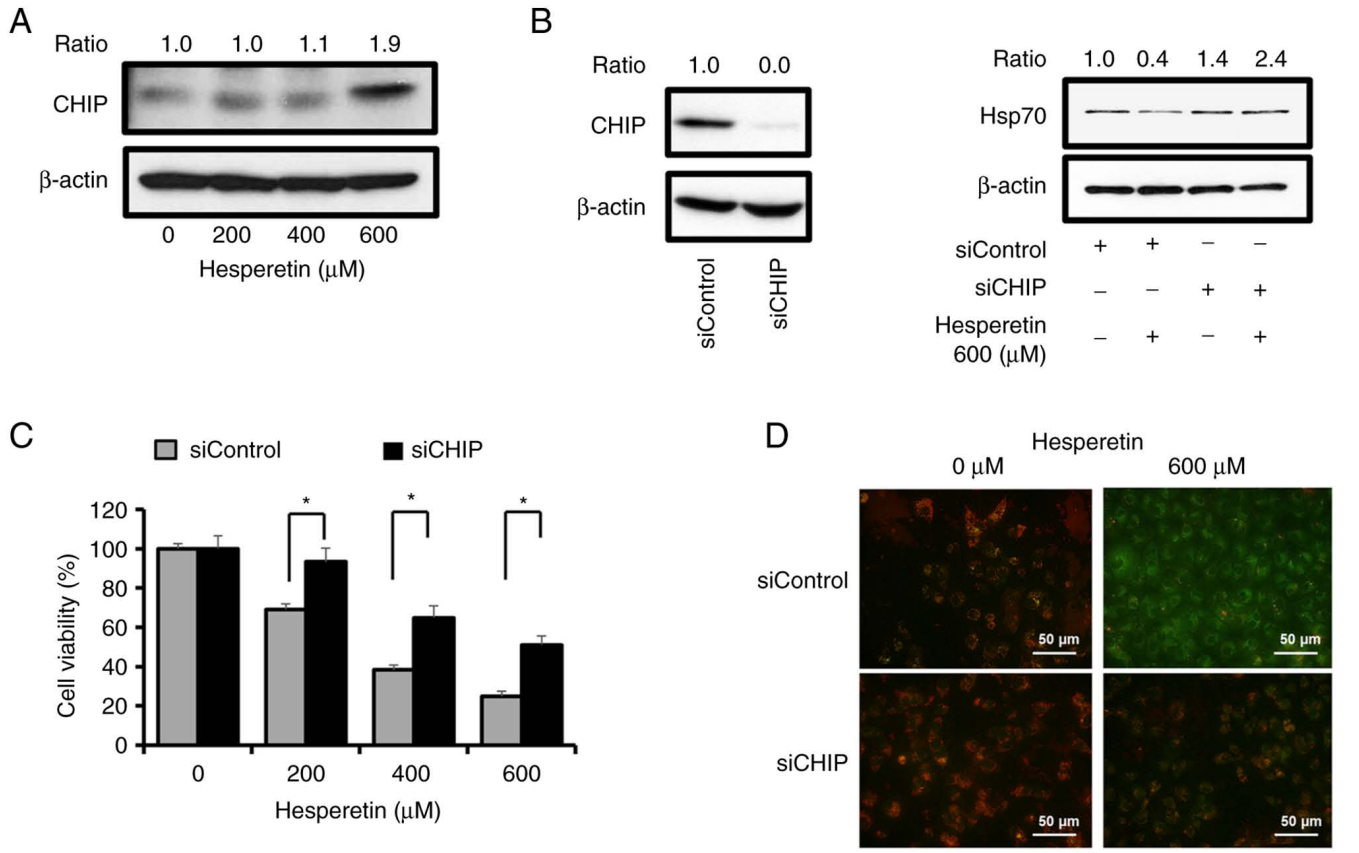

Figure 5. CHIP is involved in the proteasome-mediated degradation of Hsp70 induced by hesperetin. (A) Effect of hesperetin on CHIP expression. A549 cells were treated with various concentrations of hesperetin for 48 h. The expression of CHIP was assessed by immunoblotting using an anti-CHIP antibody. Ratios of CHIP band intensities normalized to β-actin band intensities are shown above the blots. (B) A549 cells were treated with 10 nM siRNA against CHIP or control siRNA. CHIP silencing efficiency (left panel) and its effect on Hsp70 expression (right panel) were examined by immunoblotting. Ratios of CHIP and Hsp70 band intensities normalized to β-actin band intensities are shown above the blots. Results shown are representative of three separate experiments. (C) Effect of CHIP RNAi on the viability of A549 cells treated with hesperetin. After being treated with 10 nM siRNA against CHIP or control siRNA for 72 h, A549 cells were exposed to various concentrations of hesperetin for 48 h, and the viabilities of cells were analyzed by MTT assay. Cell viability is represented as the percentage of cell viability without hesperetin treatment, which was set at 100%. Data are presented as mean ± SD from triplicated experiments. The results shown are representative of three separate experiments. *P<0.01. (D) Effect of CHIP RNAi on the mitochondria-dependent apoptosis of A549 cells treated with hesperetin. A549 cells treated with 10 nM siRNA against CHIP or control siRNA were cultured in the absence or presence of 600 μM hesperetin for 48 h and subjected to JC-1 staining to study the changes in mitochondrial membrane potential. The cells were visualized by immunofluorescence microscopy with the red and green channels. A representative experiment out of three performed with similar results is shown. Scale bar, 50 μm. Hsp70, heat shock protein 70; CHIP, C-terminus of Hsp70-interacting protein; siRNA, small interfering RNA.

staining used to determine the mitochondria-dependent apoptosis of A549 cells after treatment with hesperetin (Fig. 5D). These results clearly demonstrated the critical role of CHIP in the induction of hesperetin-mediated apoptosis in A549 cells.

Discussion

Epidemiological studies have indicated an inverse association between the dietary consumption of flavonoids and the risk of various illnesses, such as cardiovascular diseases, metabolic diseases, and cancer (15,38,39). Recently, more attention has been paid to the anticancer effects of hesperetin. Hesperetin was demonstrated to inhibit carcinogenesis in preclinical experiments using various cancer cells, including breast, lung, gastric, colon, and hepatic cancer cells (19,22-24,33). The most attractive feature of hesperetin is its broad application for a new promising class of anticancer therapeutic agents from functional food with few side effects, since it is toxic to cancer cells but not to normal cells as compared with currently available cytotoxic drugs (40,41). One widely known anticancer effect of hesperetin on cancer cells is the activation of the apoptosis pathway. Although the induction of apoptosis by hesperetin is well established, the detailed mechanisms and pathways by which this phenomenon occurs remain unknown. To link this hesperetin-dependent event mechanistically, the action of Hsp70 in apoptosis induced by hesperetin was explored. Hesperetin significantly decreased Hsp70 expression in lung adenocarcinoma cell lines and induced the apoptosis of A549 cells. This finding is fundamentally consistent with previous studies, which revealed that functionally related small molecules that inhibit Hsp70 decrease the viability of colorectal or pancreatic cancer cells by promoting apoptosis via the downregulation of Hsp70 (6,12,13). To the best of our knowledge, the present study is the first to demonstrate the involvement of Hsp70 in hesperetin-induced cell death. This observation is important because targeting the expression or function of Hsp70 is a potential treatment strategy for several types of cancer, considering the hypothesis that a high level of Hsp70 protects against cell death and increases the survival of cells exposed to apoptotic stimuli (27,42). Previous research

identified Hsp70 as a putative oncogene whose upregulation is common and driven by its genomic amplification in cancer cells (5-7), and increased Hsp70 expression is positively associated with the advanced pathologic stage and grade of cancers and related to poor outcomes of patients (8-10). These notions offer an attractive opportunity for therapeutic approaches that inhibit Hsp70. The inhibitory effects of hesperetin on Hsp70 may be supported by previous research which demonstrated that the flavonoid quercetin decreases Hsp70 expression in human cancer cell lines (11).

Several studies have indicated that activation of the mitochondrial pathway is a critical event in apoptosis induced by hesperetin (19,20,22,23,33), whereas another study reported that hesperetin induces apoptosis in cancer cells via a mitochondria-independent pathway (24). This discrepancy may be due to the different experimental systems used to evaluate apoptosis or reflects the variability of apoptotic pathways among different cell lines. In the present study, hesperetin facilitated the translocation of proapoptotic Bax to the mitochondria, and the events occurred up- and downstream of mitochondrial disruption in A549 cells. The key regulators of apoptosis, including members of the antiapoptotic and proapoptotic Bcl-2 family, affect the outer membrane permeability of the mitochondria (43). In fact, reduced expression of death-inducing members (Bax) vs. increased expression of death-inhibitory members (Bcl-2, Bcl-xL) has been reported in various cancer types and malignancies (44). Bax generally plays an important role in inhibiting the progression of cancer and promoting the apoptosis of some types of cancers. Interestingly, earlier studies have shown that hesperetin increases Bax expression in cancer cells (20,22,33), although the specific mechanisms modulating the activation of Bax remain unknown. In the present study, overexpression of Hsp70, which actively sequestrates Bax in the cytosol to interfere with its translocation to the mitochondria, rescued A549 cells from hesperetin. This result suggests that Hsp70 acts as an inhibitory molecule for the activation of Bax in hesperetin-mediated apoptosis. To clarify the mechanisms underlying the hesperetin-induced downregulation of Hsp70, it was further demonstrated that the degradation of Hsp70, associated with the upregulation of CHIP in the ubiquitin proteasome pathway, is a critical event in apoptosis induced by hesperetin. Hsp70 becomes very stable and accumulates at very high levels in cancer cells, which is a feature of the gain-of-function in tumorigenesis and cancer progression (5-7). In addition, Hsp70 is generally regulated mainly and maintained at basal levels under normal physiological conditions (45,46). Hsp70 stability is regulated by proteasome-mediated degradation through the E3 ubiquitin ligase CHIP. Previous studies have indicated the importance of CHIP-mediated Hsp70 turnover for the regulatory mechanism of Hsp70 (33,34). The lack of an inhibitory effect on Hsp70 expression and an anti-proliferative effect by hesperetin in A549 cells treated with CHIP dsRNA clearly indicate that CHIP is a notable target for the induction of hesperetin-mediated apoptosis. Based on these findings, a mechanism model for hesperetin-mediated apoptosis is proposed, as summarized in Fig. 6. Collectively, the present study provided the first evidence that Hsp70 is critical for determining the cellular decision to either initiate or suppress apoptosis mediated by hesperetin. These findings may contribute toward the development of new and less toxic chemotherapies that use natural compounds against cancer, and they also highlight the putative merits of developing anticancer treatments targeting Hsp70.

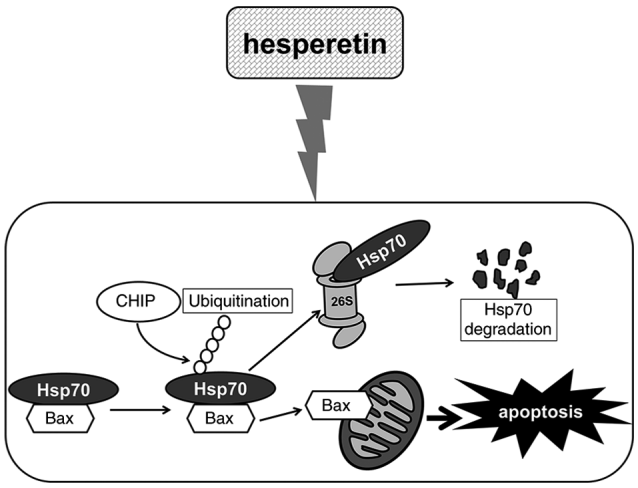

Figure 6. Schematic diagram of the mechanism underlying hesperetin-mediated apoptosis in A549 cells. Hesperetin induces the proteasome-mediated degradation of Hsp70 by increasing CHIP, leading the enhancement of Bax translocation to the mitochondria and the activation of the intrinsic mitochondria-mediated apoptosis pathway. Hsp70, heat shock protein 70; CHIP, C-terminus of Hsp70-interacting protein.

Acknowledgements

We would like to thank Dr Tohru Ichimura (Laboratory of Cell Molecular Biology, Department of Applied Chemistry, National Defense Academy, Japan) for providing the myc-Hsp70 construct.

Funding

The present study was supported by the JSPS Grants-in Aid for Scientific Research (grant nos. 19K059932 and 18K05536).

Availability of data and materials

The datasets used during the present study are available from the corresponding author upon reasonable request.

Authors' contributions

MY and HE designed the research and experiments, and supervised the experimental analysis. MT contributed to the design and implementation of the research. MT and KS carried out the experiments. MT performed the cell viability assay and prepared the samples and characterized them by flow cytometry. KS performed almost all of the other experiments. MT, HE, KS and MY analyzed the data of this study. HE supervised MT and KS who investigated the findings of this study. MY and HE confirm the authenticity of all raw data. MY wrote the paper with input from all the authors. All authors discussed the results. All authors read and approved the final manuscript.

Ethics approval and consent to participate

Not applicable.

Patient consent for publication

Not applicable.

Competing interests

The authors declare that they have no competing interests.

References

1. Hanahan D and Weinberg RA: The hallmarks of cancer. Cell 100: 57-70, 2000.
2. Nakano K and Vousden KH: PUMA, a novel proapoptotic gene, is induced by p53. Mol Cell 7: 683-694, 2001.
3. Igney FH and Krammer PH: Death and anti-death: Tumour resistance to apoptosis. Nat Rev Cancer 2: 277-288, 2002.
4. Endo H, Inoue I, Masunaka K, Tanaka M and Yano M: Curcumin induces apoptosis in lung cancer cells by 14-3-3 protein-mediated activation of Bad. Biosci Biotechnol Biochem 84: 2440-2447, 2020.
5. Jäättelä M: Escaping cell death: Survival proteins in cancer. Exp cell Res 248: 30-43, 1999.
6. Aghdassi A, Phillips P, Dudeja V, Dhaulakhandi D, Sharif R, Dawra R, Lerch MM and Saluja A: Heat shock protein 70 increases tumorigenicity and inhibits apoptosis in pancreatic adenocarcinoma. Cancer Res 67: 616-625, 2007.
7. Endo H, Yano M, Okumura Y and Kido H: Ibuprofen enhances the anticancer activity of cisplatin in lung cancer cells by inhibiting the heat shock protein 70. Cell Death Dis 5: e1027, 2014.
8. Ciocca DR, Clark GM, Tandon AK, Fuqua SA, Welch WJ and McGuire WL: Heat shock protein hsp70 in patients with axillary lymph node-negative breast cancer: Prognostic implications. J Natl Cancer Res 85: 570-574, 1993.
9. Cornford PA, Dodson AR, Parsons KF, Desmond AD, Woolfenden A, Fordham M, Neoptolemos JP, Ke Y and Foster CS: Heat shock protein expression independently predicts clinical outcome in prostate cancer. Cancer Res 60: 7099-7105, 2000.
10. Vargas-Roig LM, Gago FE, Tello O, Aznar JC and Ciocca DR: Heat shock protein expression and drug resistance in breast cancer patients treated with induction chemotherapy. Int J Cancer 79: 468-475, 1998.
11. Hosokawa N, Hirayoshi K, Nakai A, Hosokawa Y, Marui N, Yoshida M, Sakai T, Nishino H, Aoike A, Kawai K, *et al*: Flavonoids inhibit the expression of heat shock proteins. Cell Struct Funct 15: 393-401, 1990.
12. Yokota S, Kitahara M and Nagata K: Benzylidene lactam compound, KNK437, a novel inhibitor of acquisition of thermotolerance and heat shock protein induction in human colon carcinoma cells. Cancer Res 60: 2942-2948, 2000.
13. Westerheide SD, Kawahara TL, Orton K and Morimoto RI: Triptolide, an inhibitor of the human heat shock response that enhances stress-induced cell death. J Biol Chem 281: 9616-9622, 2006.
14. Parhiz H, Roohbakhsh A, Soltani F, Rezaee R and Iranshahi M: Antioxidant and anti-inflammatory properties of the citrus flavonoids hesperidin and hesperetin: An updated review of their molecular mechanisms and experimental models. Phytother Res 29: 323-331, 2015.
15. Scoditti E: Neuroinflammation and neurodegeneration: The promising protective role of the citrus flavanone hesperetin. Nutrients 12: 2336, 2020.
16. Aranganathan S and Nalini N: Antiproliferative efficacy of hesperetin (citrus flavanoid) in 1,2-dimethylhydrazine-induced colon cancer. Phytother Res 27: 999-1005, 2013.
17. Choi EJ: Hesperetin induced G1-phase cell cycle arrest in human breast cancer MCF-7 cells: Involvement of CDK4 and p21. Nutr Cancer 59: 115-119, 2007.
18. Nalini N, Aranganathan S and Kabalimurthy J: Chemopreventive efficacy of hesperetin (citrus flavonone) against 1,2-dimethylhydrazine-induced rat colon carcinogenesis. Toxicol Mech Methods 22: 397-408, 2012.
19. Palit S, Kar S, Sharma G and Das PK: Hesperetin induces apoptosis in breast carcinoma by triggering accumulation of ROS and activation of ASK1/JNK pathway. J Cell Physiol 230: 1729-1739, 2015.
20. Li Q, Miao Z, Wang R, Yang J and Zhang D: Hesperetin induces apoptosis in human glioblastoma cells via p38 MAPK activation. Nutr Cancer 72: 538-545, 2020.
21. Patel PN, Yu XM, Jaskula-Sztul R and Chen H: Hesperetin activates the Notch1 signaling cascade, causes apoptosis, and induces cellular differentiation in anaplastic thyroid cancer. Ann Surg Oncol 21 (Suppl 4): S497-S504, 2014.
22. Zhang J, Song J, Wu D, Wang J and Dong W: Hesperetin induces the apoptosis of hepatocellular carcinoma cells via mitochondrial pathway mediated by the increased intracellular reactive oxygen species, ATP and calcium. Med Oncol 32: 101, 2015.
23. Roohbakhsh A, Parhiz H, Soltani F, Rezaee R and Iranshari M: Molecular mechanisms behind the biological effects of hesperidin and hesperetin for the prevention of cancer and cardiovascular diseases. Life Sci 124: 64-74, 2015.
24. Elango R, Athinarayanan J, Subbarayan VP, Lei DKY and Alshatwi AA: Hesperetin induces an apoptosis-triggered extrinsic pathway and a p53-independent pathway in human lung cancer H522 cells. J Asian Nat Prod Res 20: 559-569, 2018.
25. Gabai VL, Meriin AB, Mosser DD, Caron AW, Rits S, Shifrin VI and Sherman MY: Hsp70 prevents activation of stress kinases. A novel pathway of cellular thermotolerance. J Biol Chem 272: 18033-18037, 1997.
26. Park HS, Cho SG, Kim CK, Hwang HS, Noh KT, Kim MS, Huh SH, Kim MJ, Ryoo K, Kim EK, *et al*: Heat shock protein hsp72 is a negative regulator of apoptosis signal-regulating kinase 1. Mol Cell Biol 22: 7721-7730, 2002.
27. Mosser DD and Morimoto RI: Molecular chaperones and the stress of oncogenesis. Oncogene 23: 2907-2918, 2004.
28. Beere HM, Wolf BB, Cain K, Mosser DD, Mahboubi A Kuwana T, Tailor P, Morimoto RI, Cohen GM and Green DR: Heat-shock protein 70 inhibits apoptosis by preventing recruitment of procaspase-9 to the Apaf-1 apoptosome. Nat Cell Biol 2: 469-475, 2000.
29. Saleh A, Srinivasula SM, Balkir L, Robbins PD and Alnemri ES: Negative regulation of the Apaf-1 apoptosome by Hsp70. Nat Cell Biol 2: 476-483, 2000.
30. Gotoh T, Terada K, Oyadomari S and Mori M: hsp70-DnaJ chaperone pair prevents nitric oxide- and CHOP-induced apoptosis by inhibiting translocation of Bax to mitochondria. Cell Death Differ 11: 390-402, 2004.
31. Stankiewicz AR, Lachapelle G, Foo CZ, Radicioni SM and Mosser DD: Hsp70 inhibits heat-induced apoptosis upstream of mitochondria by preventing Bax translocation. J Biol Chem 280: 38729-38739, 2005.
32. Livak KJ and Schmittgen TD: Analysis of relative gene expression data using real-time quantitative PCR and the 2(-Delta Delta C(T)) method. Methods 25: 402-408, 2001.
33. Zhang J, Wu D, Vikash, Song J, Wang J, Yi J and Dong W: Hesperetin induces the apoptosis of gastric cancer cells via activating mitochondrial pathway by increasing reactive oxygen species. Dig Dis Sci 60: 2985-2995, 2015.
34. Parry N, Wheadon H and Copland M: The application of BH3 mimetics in myeloid leukemias. Cell Death Dis 12: 222, 2021.
35. Los M, Mozoluk M, Ferrari D, Stepczynska A, Stroh C, Renz A, Herceg Z, Wang ZQ and Schulze-Osthoff K: Activation and caspase-mediated inhibition of PARP: A molecular switch between fibroblast necrosis and apoptosis in death receptor signaling. Mol Biol Cell 13: 978-988, 2002.
36. Qian SB, McDonough H, Boellmann F, Cyr DM and Patterson C: CHIP-mediated stress recovery by sequential ubiquitination of substrates and Hsp70. Nature 440: 551-555, 2006.
37. Kundrat L and Regan L: Identification of residues on Hsp70 and Hsp90 ubiquitinated by the cochaperone CHIP. J Mol Biol 395: 587-594, 2010.
38. Tresserra-Rimbau A, Medina-Remón A, Pérez-Jiménez J, Martínez-González MA, Covas MI, Corella D, Salas-Salvadó J, Gómez-Gracia E, Lapetra J, Arós F, *et al*: Dietary intake and major food sources of polyphenols in a Spanish population at high cardiovascular risk: The PREDIMED study. Nutr Metab Cardiovasc Dis 23: 953-959, 2013.
39. Chun OK, Chung SJ and Song WO: Estimated dietary flavonoid intake and major food sources of U.S. adults. J Nutr 137: 1244-1252, 2007.

40. Chen X, Wei W, Li Y, Huang J and Ci X: Hesperetin relieves cisplatin-induced acute kidney injury by mitigating oxidative stress, inflammation and apoptosis. Chem Biol Interact 308: 269-278, 2019.
41. He P, Ma J, Liu Y, Deng H and Dong W: Hesperetin promotes cisplatin-induced apoptosis of gastric cancer in vitro and in vivo by upregulating PTEN expression. Front Pharmacol 11: 1326, 2020.
42. Schmitt E, Gehrmann M, Brunet M, Multhoff G and Garrido C: Intracellular and extracellular functions of heat shock proteins: Repercussions in cancer therapy. J Leu Biol 81: 15-27, 2007.
43. Yang J, Liu X, Bhalla K, Kim CN, Ibrado AM, Cai J, Peng TI, Jones DP and Wnag X: Prevention of apoptosis by Bcl-2: Release of cytochrome c from mitochondria blocked. Science 275: 1129-1132, 1997.
44. Ismail NI, Othman I, Abas F, H Lajis N and Naidu R: Mechanism of apoptosis induced by curcumin in colorectal cancer. Int J Mol Sci 20: 2454, 2019.
45. Feder JH, Rossi JM, Solomon J, Solomon N and Lindquist S: The consequences of expressing hsp70 in Drosophila cells at normal temperatures. Genes Dev 6: 1402-1413, 1992.
46. Volloch VZ and Sherman MY: Oncogenic potential of Hsp72. Oncogene 18: 3648-3651, 1999.